Science Advances
AAAS

advances.sciencemag.org/cgi/content/full/6/40/eabc4364/DC1

Supplementary Materials for

Novel self-replicating α-synuclein polymorphs that escape ThT monitoring can spontaneously emerge and acutely spread in neurons

Francesca De Giorgi, Florent Laferrière, Federica Zinghirino, Emilie Faggiani, Alons Lends, Mathilde Bertoni, Xuan Yu, Axelle Grélard, Estelle Morvan, Birgit Habenstein, Nathalie Dutheil, Evelyne Doudnikoff, Jonathan Daniel, Stéphane Claverol, Chuan Qin, Antoine Loquet, Erwan Bezard, François Ichas*

*Corresponding author. Email: francois.ichas@inserm.fr

Published 2 October 2020, *Sci. Adv.* **6**, eabc4364 (2020)
DOI: 10.1126/sciadv.abc4364

This PDF file includes:

Figs. S1 to S6
Tables S1 to S3

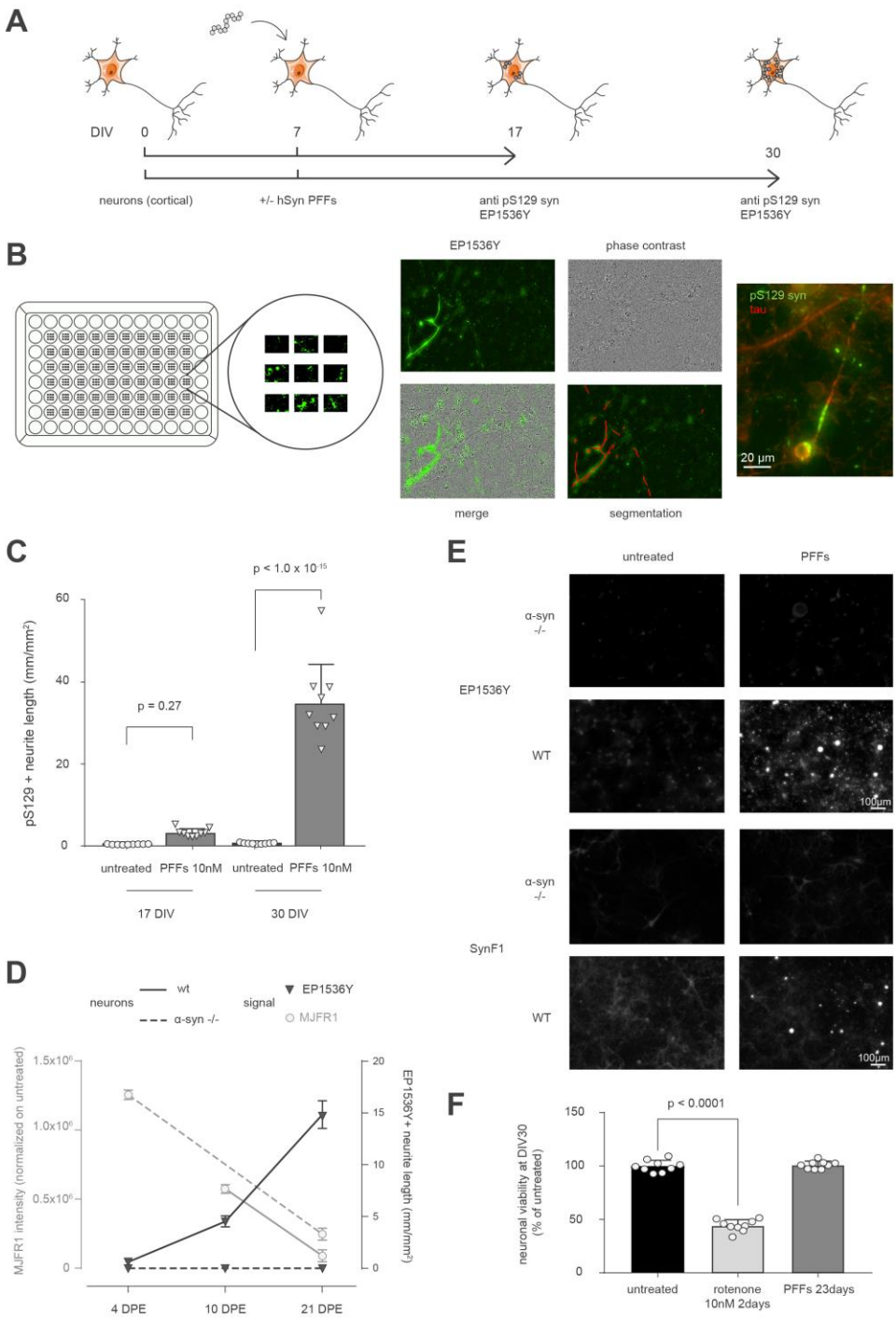

Fig. S1. High Content Analysis of experimental synucleinopathy in 96 well primary cultures of mouse cortical neurons. (A) Time schedules of the experiments shown in this figure. (B) Left: schematic view of the seeding plate map and position of the nine 20X imaging fields; Middle composite panel: representative field of acquisition with single fluorescence and phase contrast channels,

corresponding overlay, and overlay with fluorescence segmentation generated for quantitation. Right Panel: Closup of a neuron treated with 10 nM α-syn PFFs (batch 1B) from DIV7 to DIV30: pS129 syn in green and tau in red show perikaryal and neuritic synucleinopathy. (C) Quantification of the experimental synucleinopathy induced by 10 nM α-syn PFFs (batch 1B) equivalent monomer concentration at 17 and 30 days in vitro (DIV) for a common α-syn challenge with PFFs at DIV7 (n=3, 9 measurement fields per replicate, data points: inter-replicate mean of randomly matched fields). The statistical significance of the comparisons was computed using ANOVA. (D) Monitoring of the progressive degradation of the exogenous α-syn PFFs (MJFR1 positive) and of the concomitant buildup of the neuronal synucleinopathy (EP1536Y positive) in WT and α-syn (-/-) neurons. No synucleinopathic buildup takes place in neurons form α-syn (-/-) mice (Envigo) (DPE: days post PFFs exposure) (n=3, 9 measurement fields per replicate, data points: mean of 27 fields). (E) The synucleinopathy revealed by EP1536Y is also positive for the conformation-dependent amyloid-specific Syn-F1 antibody and corresponds to the recruitment of endogenous α-syn into neo-formed amyloids that get phosphorylated at S129. (F) Neuronal viability assay (calcein retention) reveals that the synucleinopathic build-up is not associated with a measurable neuronal viability decrease at DIV30 while a two-days-treatment with 10nM rotenone (from DIV28 to DIV30) induces a ~50% viability drop (n=3, 9 measurement fields per replicate, data points: inter-replicate mean of randomly matched fields). All the HCA experiments described in the main text were analysed at DIV30.

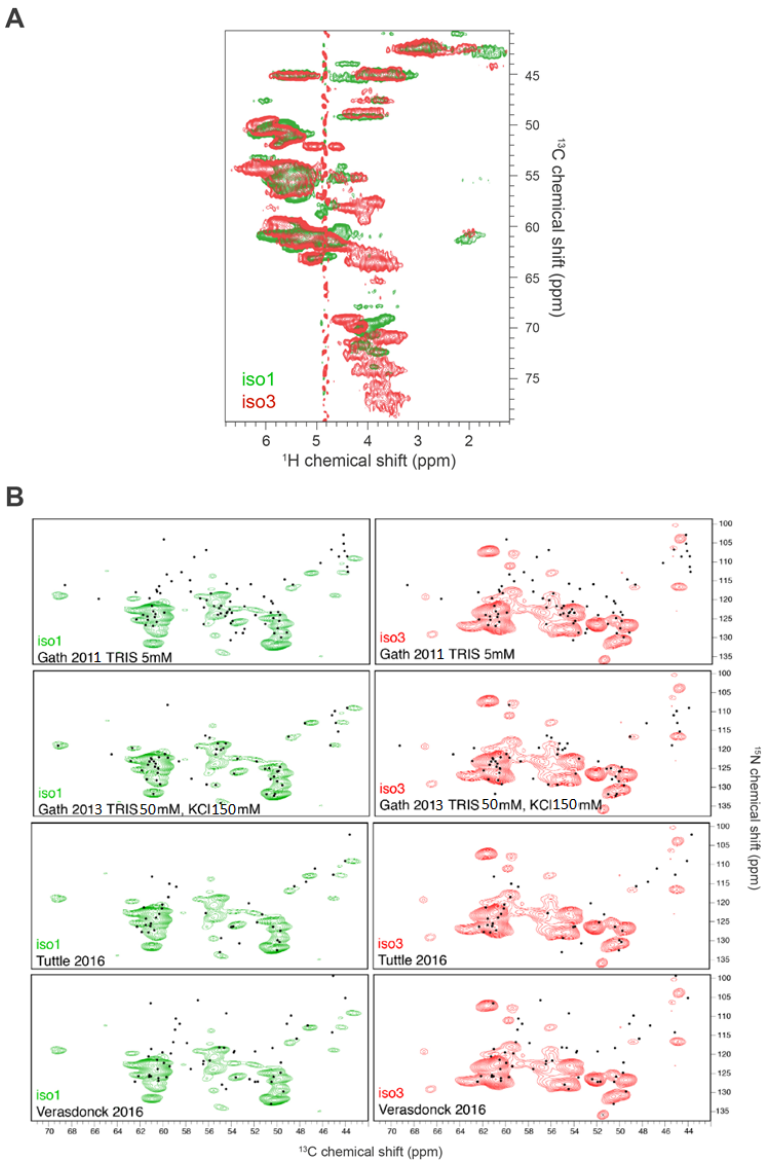

Fig. S2. Solid State NMR. (A) Solid-state NMR 2D hCH experiments of fully protonated iso1 and iso3 showing that they correspond to two distinct polymorphs. **(B)** Comparison of the 2D NCa projection for the 3D hCaNH experiments of iso1 (in green) and iso3 (in red) with reported chemical shift resonances (black dots) of the α-syn fibril polymorphs from references 13 to 16. Note that iso1 is equivalent to the type 2 fibril polymorph (*14, 18*). According to the classification of Ref. 18: Tuttle 2016 and Verasdonck 2016 = Type 1; Gath 2013 = Type 2, Gath 2011 = neither Type 1 nor Type 2 (also known as as "Ribbons").

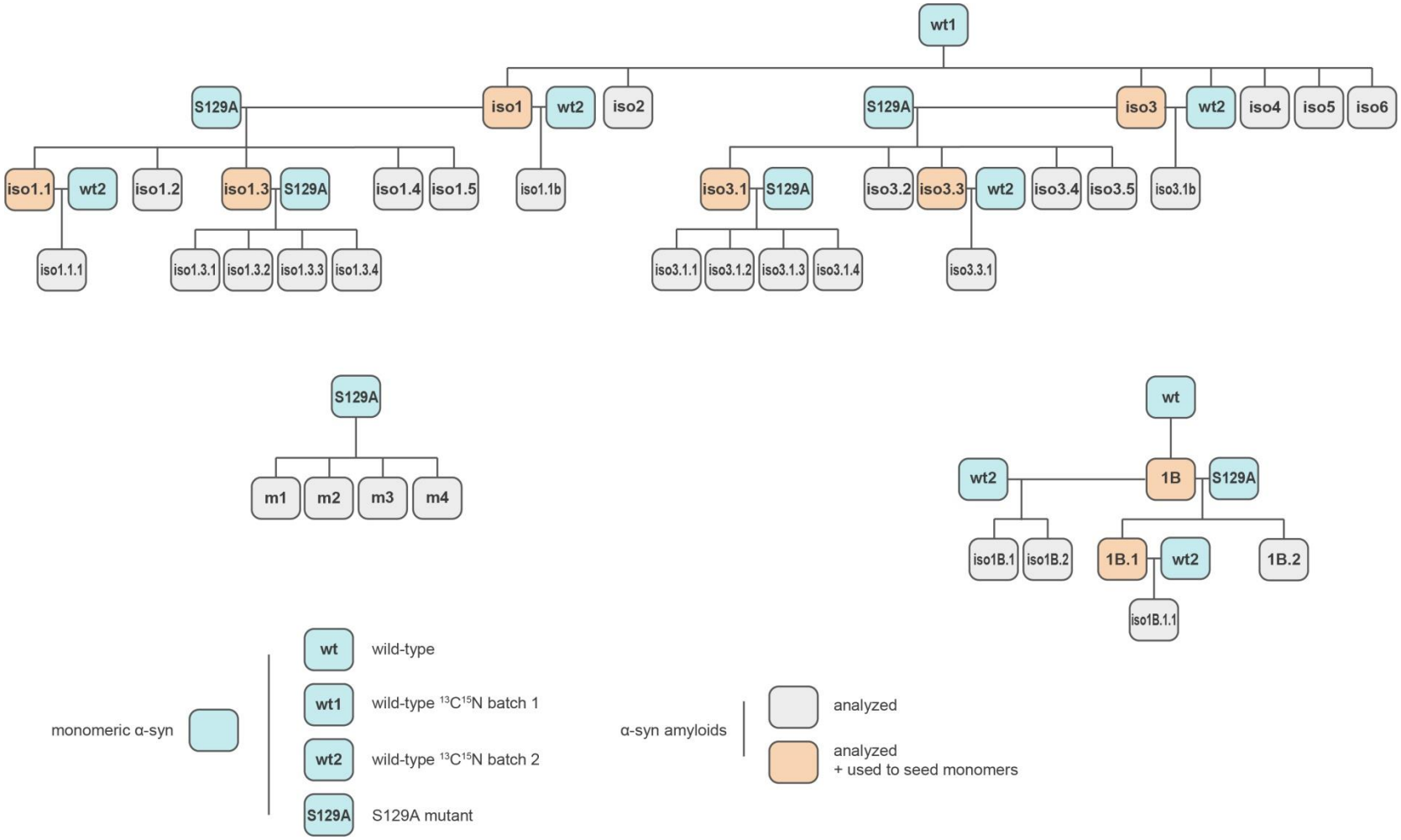

Fig. S3. Complete genealogy of the α-syn amyloid polymorphs used in this study.

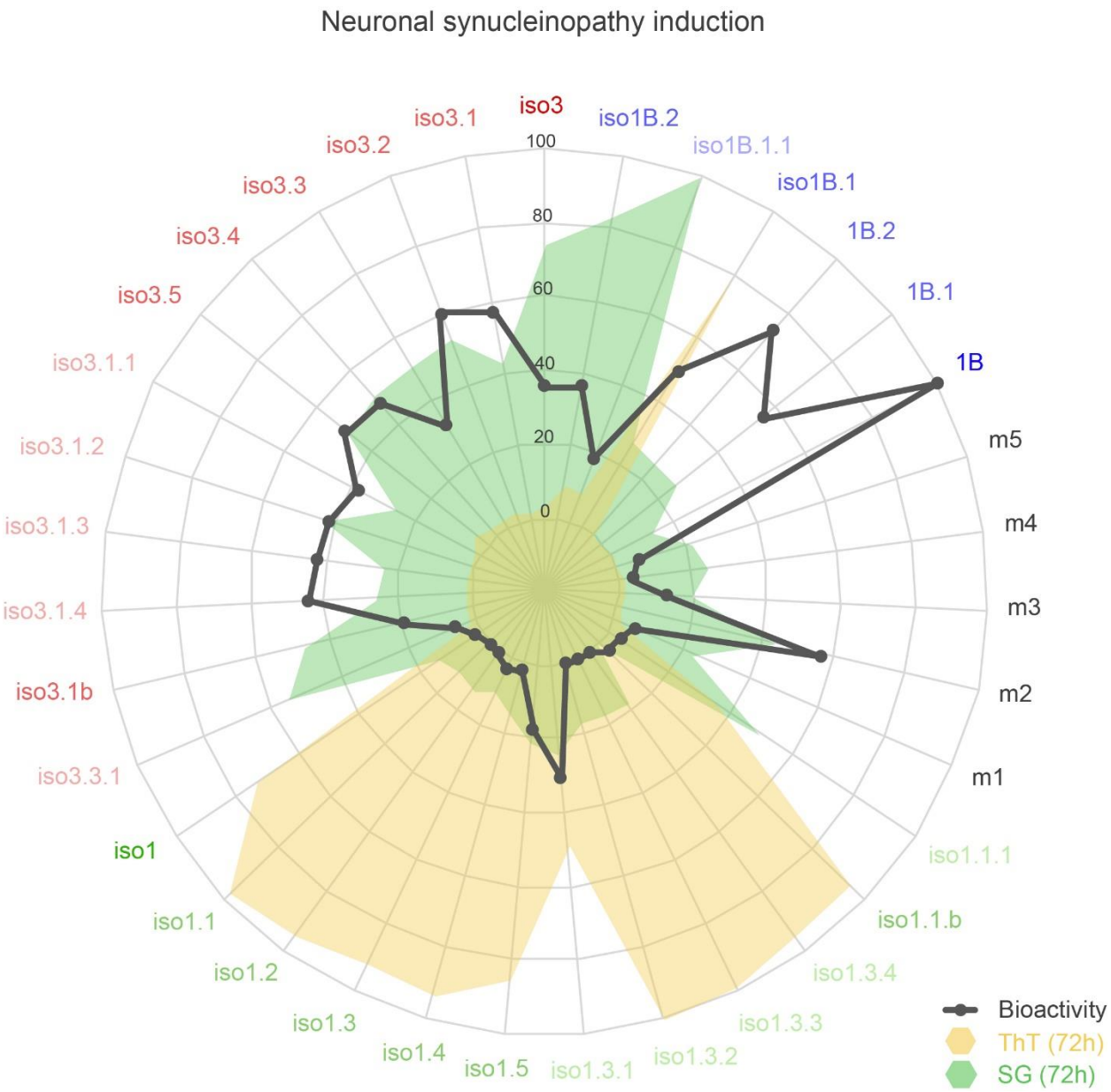

Fig. S4. Radar plot of the ThT, SG and neuronal bioactivity values. The members of the genealogy of Fig. S3 and the spontaneous fibrillizations m1 to m5 are shown. For each sample, the three variables were divided by the X-34 value of the sample to normalize the data with respect to the total amyloid contents of the sample.

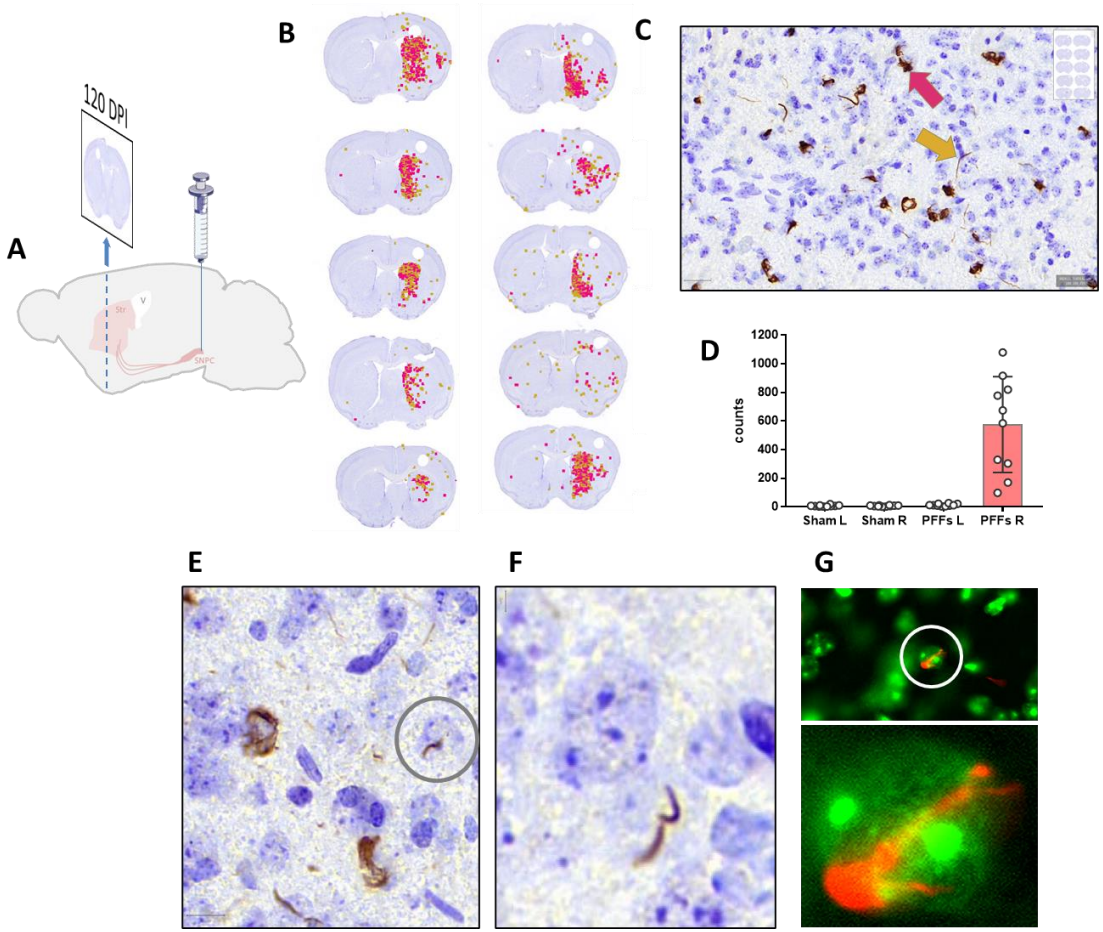

Fig. S5. The τ⁻ polymorph 1B triggers a synucleinopathy that spreads from the substantia nigra to the striatum *in vivo*. Ten wild-type mice were stereotaxically injected at the level of their right subtantia nigra, pars compacta, with τ⁻ polymorph fibrils 1B (A). At 120 days post injection (DPI), immunohistochemistry of rostral brain sections (Bregma + 0.6 to + 0.8 mm, V: ventricle) sampling

the striatum reveals the presence of EP1536Y-positive α-syn aggregates taking the form of somatic aggregates/tangles (in B: red dots, in C: red arrow) or of Lewy neurites (in B: yellow dots, in C: yellow arrow). B: distribution of the synucleinopathy in the same sectioning plane for each animal and C: higher magnification demonstrating the cytological typology of the synucleinopathy. D: total count of somatic aggregates plus Lewy neurites in the left (not injected) and right (injected) hemi-sections of 10 sham-injected animals and of the 10 PFFs-injected ones. In agreement with the *in vitro* observations, and besides somatic aggregates/tangles and Lewy neurites, PFFs 1B also induced the appearance of neuronal nuclear inclusions that were EP1536Y-positive. E and F show 2 different examples of such inclusions revealed by IHC against the cresyl counterstain, and G shows two magnifications of an EP1536Y positive intranuclear inclusion revealed by IF (red) against the DNA-intercalating probe DAPI (color-coded in green for better visibility).

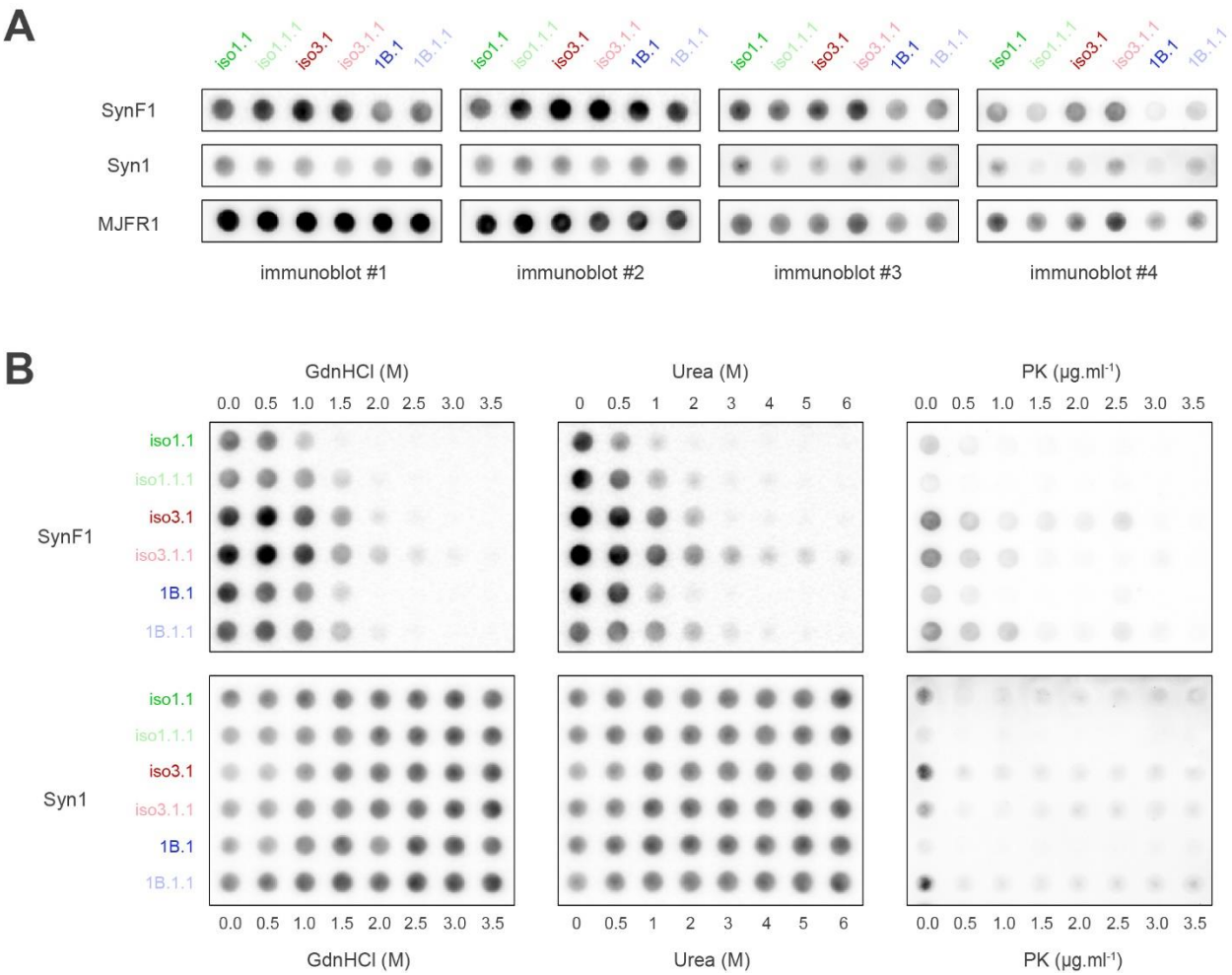

Fig. S6. Representative immunoblots of filter trap assays used for the assessment of the fibril immunoreactivity and resistance to disassembly, denaturation and proteolysis. (A) Untouched iso1.1 (dark green), iso1.1.1 (light green), iso3.1 (dark red), iso3.1.1 (light red), 1B.1 (dark blue) and 1B.1.1 (light blue) fibrillar recombinant human α-synuclein preparations were subjected to filter trap assays followed by immunoblotting with antibodies against aggregated (SynF1), monomeric (Syn1) and total human (MJFR1) α-syn. The signal intensities and their ratios were used for quantifying the immunoreactivity of each type of assembly to SynF1. (B) The same fibrillar preparations were treated with indicated increasing concentrations of GdnHCl (1 hour at room temperature), Urea (6 hours at room temperature), and Proteinase K (30 minutes

at 37°C). Each sample was subjected to filter trap assay immunoblotted with SynF1 and Syn1 antibodies in order to quantify the disappearance of fibrillar, and the appearance of monomeric α-synuclein forms respectively. The signals normalized to untreated samples allowed the assessment of the resistance of each fibril type to disassembly, denaturation and proteolysis.

Table S1. List of the Antibodies used in this study

Antibody	Target	Company	Cat.No	Dilution IF	Dilution IB
Primary antibodies					
MJFR-1	human alpha-synuclein	Abcam	ab138501	1 : 1 000	1 : 10 000
EP1536Y	pS129 phospho-synuclein	Abcam	ab51253	1 : 500	1 : 5 000
Syn1 clone 42	monomeric alpha-synuclein	BD Biosciences	610787	1 : 500	1 : 2 000
Syn-F1	aggregated alpha-synuclein	BioLegend	847802	1 : 500	1 : 10 000
T46	tau	Thermo Fisher Scientific	13-6400	1 : 500	n/a
Actin	beta-actin	Sigma	A5316	n/a	1 : 10 000
Secondary antibodies					
Goat anti-mouse HRP	Mouse IgG (H+L)	Jackson Immuno Research	115-035-146	n/a	1 : 10 000
Goat anti-rabbit HRP	Rabbit IgG (H+L)	Jackson Immuno Research	111-035-144	n/a	1 : 10 000
Donkey anti-mouse Alexa 488	Mouse IgG (H+L)	Thermo Fisher Scientific	A-21202	1 : 500	n/a
Goat anti-rabbit Alexa 488	Rabbit IgG (H+L)	Thermo Fisher Scientific	A-11008	1 : 500	n/a
Donkey anti-mouse Alexa 594	Mouse IgG (H+L)	Thermo Fisher Scientific	A-21203	1 : 500	n/a
Donkey anti-rabbit Alexa 594	Rabbit IgG (H+L)	Thermo Fisher Scientific	A-21207	1 : 500	n/a

Table S2. The Solid-state NMR parameters for 2D spectra.

	Polymorph 1		Polymorph 3	
Experiment	**2D hNH**	**2D hCH**	**2D hNH**	**2D hCH**
MAS frequency/kHz	100	100	100	100
Field/T	18.8	18.8	18.8	18.8
Transfer I	HN-CP	HC-CP	HN-CP	HC-CP
^{1}H field/kHz	80	80	80	80
^{15}N field/kHz	20		20	
^{13}C field/kHz		20		20
Shape	ramp ^{1}H	ramp ^{1}H	ramp ^{1}H	ramp ^{1}H
Time/ms	1.5	0.3	0.9	0.3
Transfer II	NH-CP	CH-CP	NH-CP	CH-CP
^{1}H field/kHz	80	80	80	80
^{15}N field/kHz	20		20	
^{13}C field/kHz		20		20
Shape	ramp ^{1}H	ramp ^{1}H	ramp ^{1}H	ramp ^{1}H
Time/ms	0.5	0.3	0.8	0.3
^{13}C carrier/ppm		54		54
^{1}H decoupling	slTPPM12	slTPPM12	slTPPM12	slTPPM12
^{1}H decoupling field/ kHz	25	25	25	25
t1 increments	74	300	74	300
Windows function	QSine 3	QSine 3	QSine 3	QSine 3
Sweep width (t1)/kHz	42.4	16.1	42.4	16.1
Acquisition time (t1)/ms	11.4	9.3	11.4	9.3
^{15}N/^{13}C decoupling	WALTZ16	WALTZ16	WALTZ16	WALTZ16
^{15}N/^{13}C decoupling field/ kHz	10	10	10	10
t2 increments	2048	2048	2048	2048
Windows function	QSine 3	QSine 3	QSine 3	QSine 3
Sweep width (t2)/kHz	100	37	100	37
Acquisition time (t2)/ms	10.2	27.6	10.2	27.6
Water supperession scheme	MISSISSIPPI	MISSISSIPPI	MISSISSIPPI	MISSISSIPPI
Interscan delay/s	1.3	2	1.3	2
Number of scans	64	32	64	32
Measurement time/h	2	6	2	6

Table S3. The Solid-state NMR parameters for 3D spectra.

	Polymorph 1	Polymorph 3
Experiment	**3D hCaNH**	**3D hCaNH**
MAS frequency/kHz	100	100
Field/T	18.8	18.8
Transfer I	HN-CP	HN-CP
^{1}H field/kHz	80	80
^{13}C field/kHz	20	20
Shape	ramp ^{1}H	ramp ^{1}H
Time/ms	0.9	1.1
Transfer II	CN-CP	CN-CP
^{15}N field/kHz	20	20
^{13}C field/kHz	80	80
Shape	ramp ^{15}N	ramp ^{15}N
Time/ms	10	10
^{13}C carrier/ppm	54	54
^{1}H decoupling	slTPPM12	slTPPM12
^{1}H decoupling field/ kHz	25	25
Transfer III	NH-CP	NH-CP
^{1}H field/kHz	80	80
^{15}N field/kHz	20	20
Shape	ramp ^{1}H	ramp ^{1}H
Time/ms	0.6	0.6
t1 increments	56	70
Windows function	QSine2	QSine2
Sweep width (t1)/kHz	7.6	10.4
Acquisition time (t1)/ms	3.7	3.3
^{1}H decoupling	slTPPM12	slTPPM12
^{1}H decoupling field/ kHz	25	25
t2 increments	38	46
Windows function	QSine 2	QSine 2
Sweep width (t2)/kHz	4	3.1
Acquisition time (t2)/ms	4.6	7.4
^{15}N/^{13}C decoupling	WALTZ16	WALTZ16
N/^{13}C decoupling field/ kH	10	10
t3 increments	1536	1536
Windows function	QSine 2	QSine 2
Sweep width (t1)/kHz	100	100
Acquisition time (t1)/ms	7.5	7.5
ater supperession scher	MISSISSIPPI	MISSISSIPPI
Interscan delay/s	1.2	1.3
Number of scans	44	64
Measurement time/h	31.2	74.4